THE JOURNAL OF BIOLOGICAL CHEMISTRY VOL. 286, NO. 23, pp. 20991–21001, June 10, 2011

Relationship between Complement Membrane Attack Complex, Chemokine (C-C Motif) Ligand 2 (CCL2) and Vascular Endothelial Growth Factor in Mouse Model of Laser-induced Choroidal Neovascularization*

Received for publication, January 28, 2011, and in revised form, March 23, 2011 Published, JBC Papers in Press, April 22, 2011, DOI 10.1074/jbc.M111.226266

Juan Liu[‡§], **Purushottam Jha**[‡], **Valeriy V. Lyzogubov**[‡], **Ruslana G. Tytarenko**[‡], **Nalini S. Bora**[‡§1], **and Puran S. Bora**[‡2]
From the Departments of [‡]*Ophthalmology and* [§]*Microbiology and Immunology, University of Arkansas for Medical Sciences, Little Rock, Arizona 72205*

The present study investigated the interactions among the complement membrane attack complex (MAC), CCL2, and VEGF that occur *in vivo* during the development of choroidal neovascularization (CNV). We first investigated the sequential expression of MAC, CCL2, and VEGF during laser-induced CNV in C57BL/6 mice. Increased MAC deposition was detected at 1 h, CCL2 increased at 3 h, and VEGF was up-regulated at day 3 post-laser treatment. These results suggested that during laser-induced CNV, MAC, CCL2 and VEGF are formed and/or expressed in the following order: MAC → CCL2 → VEGF. To determine the cross-talk between MAC, CCL2, and VEGF during laser-induced CNV, neutralizing antibodies were injected both systemically and locally to block the bioactivity of each molecule. Blocking MAC formation inhibited CCL2 and VEGF expression and also limited CNV formation, whereas neutralization of CCL2 bioactivity did not affect MAC deposition; however, it reduced VEGF expression and CNV formation. When bioactivity of VEGF was blocked, CNV formation was significantly inhibited, but MAC deposition was not affected. Together, our results demonstrate that MAC is an upstream mediator and effect of MAC on the development of laser-induced CNV can be attributed to its direct effect on VEGF as well as its effect on VEGF that is mediated by CCL2. Understanding the interplay between immune mediators is critical to gain insight into the pathogenesis of CNV.

Age-related macular degeneration (AMD)[3] is the major cause of irreversible blindness in individuals over the age of 50 worldwide (1–5). Based on clinical and pathological features, AMD is usually classified into two forms: the nonexudative/dry form and the exudative/wet form (6, 7). Wet AMD is a pathological process, secondary to choroidal neovascular changes (CNV). CNV is a complex pathogenic process where new blood vessels are generated beneath the retina from pre-existing choriocapillaries (8–10). Several risk factors have been reported to be associated with CNV formation (11–15). Studies reported in the literature support a key role for the complement system in the development of CNV (16–21).

Although the complement system is recognized traditionally as a major component of innate immunity, it has multifunctional role in immunity, including the initiation and regulation of adaptive immune responses (22–26). The role of the complement in the development of CNV has been more directly addressed by using laser-induced animal model (27–29). The laser-induced model of CNV is produced in C57BL/6 mice by laser photocoagulation, and this model is used by an increasing number of investigators (29–32). Using this animal model of CNV, we demonstrated that complement activation, especially the formation of membrane attack complex (MAC), is crucial for the development of laser-induced CNV (27–29). We also reported that there is a direct correlation between MAC deposition and levels of angiogenic growth factors, including VEGF during laser-induced CNV (29).

Studies reported in the literature have indicated a possible role of chemokines such as chemokine (C-C motif) ligand 2 (CCL2) in CNV formation (33–35). However, the exact role of CCL2 in CNV formation still remains unclear. It has been reported that down-regulation of CCL2 inhibited laser-induced CNV (34), whereas another study demonstrated that aged mice deficient in CCL2 develop key features of human AMD (36). CCL2, also known as monocyte chemotactic protein-1 belongs to the CC chemokine family (37, 38). Several studies have suggested that the expression of various chemokines can be regulated by MAC, the end product of complement activation (39–42). It is also known that various chemokines can modulate the levels of angiogenic growth factors (43–46). To our knowledge, the cross-talk between MAC, chemokines, and angiogenic growth factors in laser-induced CNV has not been elucidated thus far. In the present study, we asked whether the effect of MAC on the induction and/or release of angiogenic growth factor, VEGF, is mediated via CCL2. We believe that it is important to determine the interactions between MAC, CCL2, and

* This work was supported, in whole or in part, by National Institutes of Health Grants EY014623 and EY018812. This work was also supported by grants from the Pat and Willard Walker Eye Research Center, Jones Eye Institute, and the University of Arkansas for Medical Sciences (Little Rock, AR).
[1] To whom correspondence may be addressed: Dept. of Ophthalmology, Jones Eye Institute, University of Arkansas for Medical Sciences, 4301 West Markham, 523 Little Rock, AR 72205-7199. Tel.: 501-686-8293; Fax: 501-686-8316; E-mail: NBora@UAMS.edu.
[2] To whom correspondence may be addressed: Dept. of Ophthalmology, Jones Eye Institute, University of Arkansas for Medical Sciences, 4301 West Markham, 523 Little Rock, AR 72205-7199. Tel.: 501-686-8293; Fax: 501-686-8316; E-mail: PBora@UAMS.edu.
[3] The abbreviations used are: AMD, age-related macular degeneration; MAC, membrane attack complex; CNV, choroidal neovascularization; CCL2, chemokine (C-C motif) ligand 2; β-FGF, basic fibroblast growth factors; RPE, retinal pigment epithelium; RT-qPCR, real-time quantitative RT-PCR.

VEGF that occur *in vivo* during laser-induced CNV because such studies will lead to a better understanding of the immunopathogenesis of wet AMD and are required for the development of effective therapy based on specific blockade of critical immune mediators.

EXPERIMENTAL PROCEDURES

Animals—Eight-week-old male C57BL/6 mice were purchased from The Jackson Laboratory (Bar Harbor, ME) and were maintained under pathogen-free conditions in the animal facility at the University of Arkansas for Medical Sciences. This study was approved by the Institutional Animal Care and Use Committee of the University of Arkansas for Medical Sciences (Little Rock, AR).

Antibodies—Purified IgG fractions of rabbit anti-mouse C6 (Cell Sciences, Canton, MA), monoclonal rat anti-mouse CCL2 (R&D Systems, Minneapolis, MN), and purified IgG fractions of goat anti-mouse VEGF (R&D Systems) were used. Purified normal rabbit IgG (Cell Sciences), rat IgG (R&D Systems) and goat IgG (R&D Systems) served as the control for C6, CCL2, and VEGF, respectively.

Induction and Measurement of CNV—CNV was induced by laser photocoagulation in both eyes of C57BL/6 mice with an Argon laser (50-μm spot size; 0.05-s duration; 260 milliwatt) as described previously (27–29, 47–52). Six laser spots were placed in each eye close to the optic disc. Production of a vaporization bubble at the time of laser treatment confirmed the rupture of Bruch's membrane.

Animals were anesthetized with ketamine/xylazine mixture at different time points post-laser treatment and perfused with 1 ml of PBS containing 50 mg/ml FITC-dextran (Sigma-Aldrich). Eyes were harvested and fixed in 10% phosphate-buffered formalin for 4 h, and retinal pigment epithelium (RPE)-choroid-sclera flat mounts were prepared as described previously (27–29). After blocking nonspecific binding with 1% BSA for 2 h, RPE-choroid-sclera flat mounts were incubated with the anti-elastin polyclonal antibody overnight at 4 °C (1:100 dilution; Santa Cruz Biotechnology), triple-washed with PBS, incubated with the Cy3-labeled secondary antibody for 1 h (1:200 dilution; Sigma-Aldrich), washed three times with PBS, and mounted in ProLong Gold Anti-fade Mounting Medium (Invitrogen). RPE-choroid-sclera flat mounts were examined under a ZEISS LSM 510 laser confocal microscope, and images of laser spots were captured. The *green* color in the laser spot represents the CNV complex, whereas the elastin was stained *red*. Area of green fluorescence (CNV size) was measured using the NIH ImageJ program.

In Vivo Antibody Administration—To block MAC formation, C57BL/6 mice (group 1, $n = 21$ mice) received a total of eight injections of anti-murine C6 (50 μg/injection) via the i.p. route before laser treatment on days −7, −6, −5, −4, −3, −2, and −1 and immediately after laser treatment (day 0). Control animals (group 2, $n = 21$ mice) received a similar treatment with purified normal rabbit IgG. Another group of mice (group 3, $n = 21$ mice) received a single subretinal injection of anti-C6 (1.4 μg in 2 μl) immediately after laser treatment. Control animals (group 4, $n = 21$ mice) received a similar treatment with purified normal rabbit IgG. To block the bioactivity of CCL2, C57BL/6 mice (group 5, $n = 15$ mice mice) received a total four injections of anti-murine CCL2 (100 μg/injection) via an i.p. route before laser treatment on days −2 and −1 and at 6 and 12 h post-laser treatment. Control animals (group 6, $n = 15$ mice) received a similar treatment with purified rat IgG. Another group of mice (group 7, n = 15 mice) received a single subretinal injection of anti-CCL2 (10 μg in 2 μl) immediately after laser treatment. Control animals (group 8, n = 15 mice) received a similar treatment with purified rat IgG. To block the bioactivity of VEGF, C57BL/6 mice (group 9, n = 15 mice) received total seven injections of anti-murine VEGF (100 μg/injection) via ip route on days 0 (right after laser treatment), 1, 2, 3, 4, 5, and 6 after laser treatment. Control animals (group 10, n = 15 mice) received a similar treatment with purified normal goat IgG. Another group of mice (group 11, $n = 6$ mice) received a single subretinal injection of anti-VEGF (15 μg in 2 μl) 2 days after laser treatment. Control animals (group 12, $n = 6$ mice) received a similar treatment with purified goat IgG.

Measurement of MAC Deposition—RPE-choroid-sclera flat mounts were stained for MAC with a polyclonal antibody (raised in rabbit) reactive with rat/mouse C9 (kindly provided by Professor B. P. Morgan (University of Wales College of Medicine, Cardiff, UK) at a 1:1000 dilution as described previously (27–29, 50). FITC-conjugated anti-rabbit IgG obtained from Invitrogen was used as the secondary antibody at a 1:400 dilution. After incubation, sections were covered with ProLong Gold Mounting Medium (Invitrogen). Control stains were performed with normal rabbit serum at concentrations similar to the primary antibody, and additional controls consisted of staining by omission of the primary or secondary antibody. Flat mounts were examined under confocal microscope (Zeiss LSM510) and Z-stack images (2-μm thickness of each optical section) of the laser-injured area were captured. Mean intensity of green fluorescence in area of laser injury was measured using the NIH ImageJ program in each Z-stack layer. The mean value of intensity for each laser spot was calculated. Each experiment was repeated three times.

Real-time Quantitative RT-PCR (RT-qPCR)—Animals were sacrificed at various time points post-laser treatment, and RPE-choroid tissue harvested from the enucleated eyes were pooled separately for each time point. Total RNA was purified using the RNeasy mini kit (Qiagen, Valencia, CA), and cDNA was synthesized using the iScript cDNA synthesis kit (Bio-Rad) with 0.5 μg of total RNA according to the manufacturer's recommendations. qPCR was performed with primers specific for mouse CCL2, VEGF, and GAPDH using iQ SYBR Green Supermix in an iQ5 real-time PCR detection system (Bio-Rad). The primers were designed and ordered from Integrated DNA Technologies (Coralville, IA), and primer sequences used were as follows: mouse CCL2, 5′-AACTCTCACTGAAGCCAGCTCT-3′ (forward) and 5′-CGTTAACTGCATCTGGCTGA-3′ (reverse); mouse VEGF, 5′-GTTCACTGTGAGCCTTGTTCAG-3′ (forward) and 5′-GTCACATCTGCAAGTACGTTCG-3′ (reverse); and mouse GAPDH, 5′-CTGGAGAAACCTGCCAAGTA-3′ (forward) and 5′-TGTTGCTGTAGCCGTATTCA-3′ (reverse).

Pilot real-time RT-qPCR experiments were performed to determine optimal condition for each primer. All real-time RT-

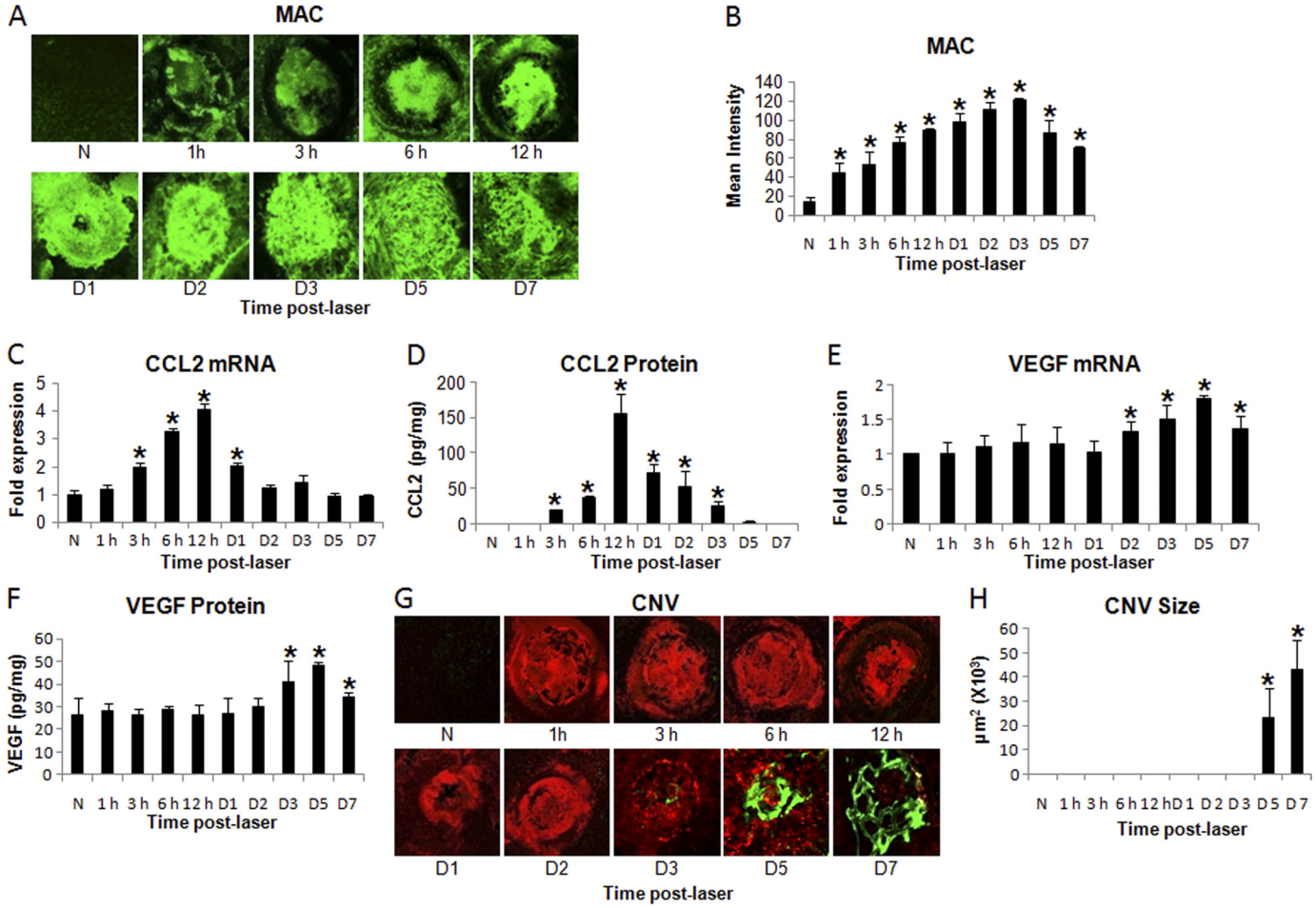

FIGURE 1. **Time-dependent expression of MAC, CCL2, and VEGF during laser-induced CNV.** CNV was induced by laser photocoagulation and C57BL/6 mice were sacrificed at various time points: 1 h, 3 h, 6 h, 12 h, day 1, day 2, day 3, day 5, and day 7 post-laser treatment. *A*, representative confocal micrographs of RPE-choroid-sclera flat mounts immunostained for MAC at various time points post-laser treatment are shown. The graph shows semi-quantitative evaluation of positive fluorescent signal for MAC (*B*). CCL2 mRNA (*C*) and protein (*D*) levels were analyzed by quantitative real-time RT-PCR and ELISA, respectively, at the time points mentioned above. Levels of VEGF mRNA (*E*) and protein (*F*) at these time points were determined by real-time RT-PCR and ELISA. CNV formation was monitored by immunohistochemical staining of RPE-choroid-sclera flat mounts, and results were quantified as described under "Experimental Procedures." Representative confocal microphotographs of RPE-choroid-sclera flat mounts from C57BL/6 mice sacrificed at different time points after laser treatment show new vessels as *green* and *red* for elastin (*G*). CNV was quantified by NIH ImageJ software and cumulative data obtained by the quantification of the images are shown in *H*. Quantification and statistical analyses, including S.D. and Student's *t* test, were performed as described under "Experimental Procedures." All data are representative of three independent experiments. *N* represents naïve mice. *, $p < 0.05$.

qPCR experiments were performed in duplicate. The primer specificity of the amplification product was confirmed by melting curve analysis of the reaction products using SYBR Green as well as by visualization on ethidium bromide-stained agarose (1.5%) gels. The housekeeping gene GAPDH was used as an internal control, and gene-specific mRNA expression was normalized against GAPDH expression. iQ^{TM}5 optical system software (Bio-Rad; version 2.0) was used to analyze real-time RT-qPCR data and derive threshold cycle (C_T) values according to the manufacturer's instructions. The DDC_T method was used to transform C_T values into relative quantities with S.D. The same software was used to calculate the normalized expression of the gene of interest, using GAPDH as reference gene, and the results were expressed as normalized fold expression.

ELISA—RPE-choroid tissue harvested from the enucleated eyes were pooled, placed in 500 μl of lysis buffer, and homogenized on ice for 30 s. The lysate was then centrifuged at 10,000 rpm for 10 min at 4 °C, and levels of CCL2 and VEGF proteins in the supernatant were determined using a mouse CCL2 and VEGF ELISA kit (both from R&D Systems), respectively. ELISA was performed according to the manufacturer's recommendations, and samples were assayed in triplicate. The concentration of each cytokine was calculated by computer software using the standard curves obtained from known concentrations (ELISA kit).

Statistical Analysis—The data are expressed as the mean ± S.D. Data were analyzed and compared using analysis of variance, and differences were considered statistically significant with $p < 0.05$.

RESULTS

A combination of following four approaches was used to establish a link between MAC, the end product of complement activation, CCL2 (chemokine), and VEGF (angiogenic growth factor) during the development of laser-induced CNV in mice.

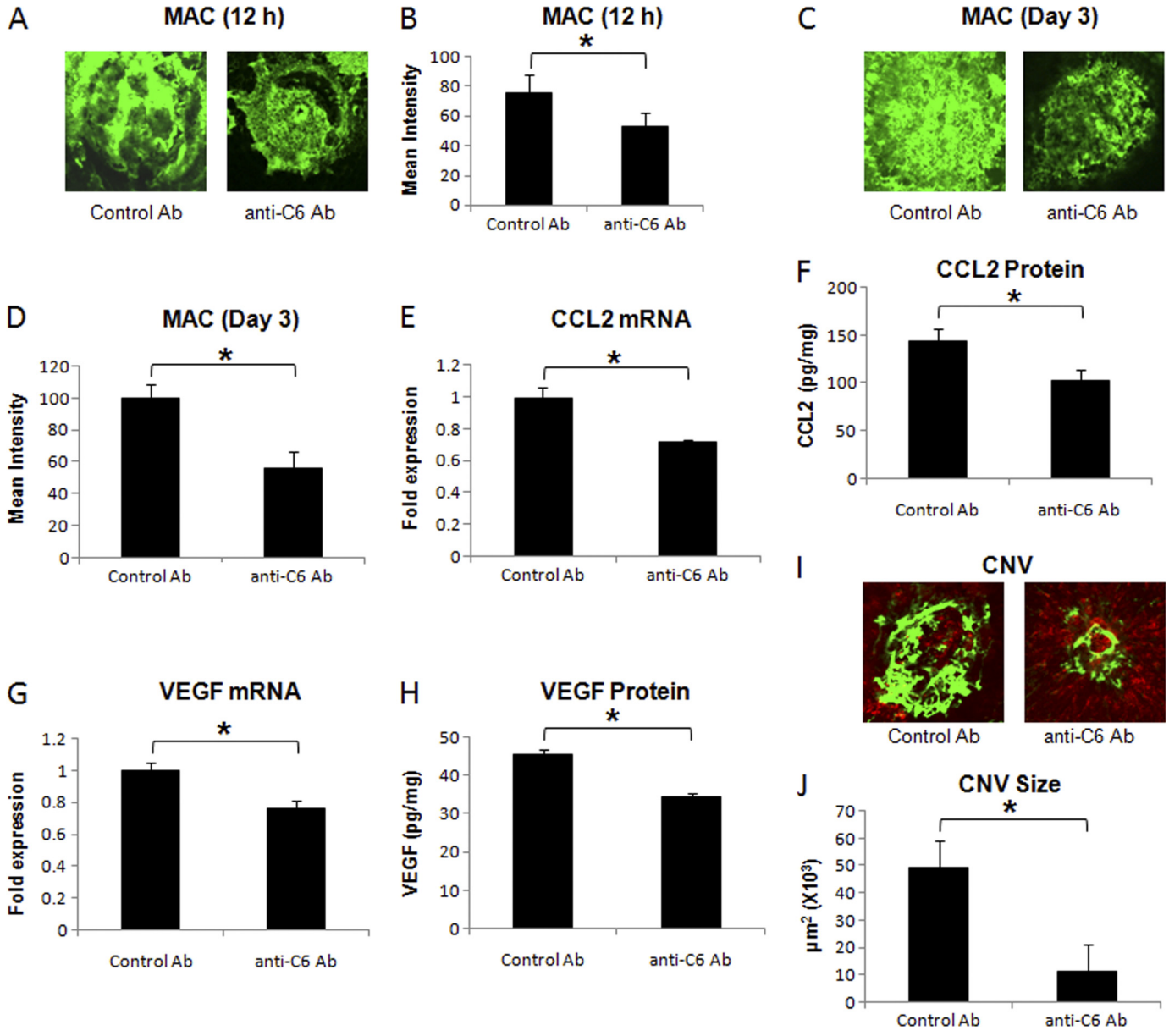

FIGURE 2. **Effect of i.p. injection of anti-murine C6 on MAC deposition, CCL2 expression, VEGF expression, and formation of CNV complex.** Representative confocal micrographs of RPE-choroid-sclera flat mounts immunostained for MAC at 12 h (*A*) and day 3 (*C*) post-laser treatment from mice injected i.p. with anti-murine C6 or control antibody. Graphs show semi-quantitative evaluation of positive fluorescent signal for MAC at 12 h (*B*) and at day 3 (*D*). CCL2 mRNA (*E*) and protein (*F*) levels were analyzed 12 h after laser treatment, whereas levels of VEGF mRNA (*G*) and protein (*H*) were determined at day 3 post-laser treatment by real-time RT-PCR and ELISA, respectively, in RPE-choroid of mice treated i.p. with anti-murine C6 or control antibody. Representative confocal microphotographs of RPE-choroid-sclera flat mounts with FITC-dextran perfused vessels (*green*) from C57BL/6 mice injected i.p. with anti-murine C6 or control antibody and sacrificed at day 7 post-laser treatment are shown (*I*). Cumulative data obtained by the quantification of the images are shown in *J*. Quantification and statistical analyses, including S.D. and Student's *t* test, were performed as described under "Experimental Procedures." All data are representative of three independent experiments. *, $p < 0.05$.

Expression Profile of MAC, CCL2, and VEGF during Laser-induced CNV

To study the sequential expression of MAC, CCL2, and VEGF, CNV was induced in C57BL/6 mice using an Argon laser. After laser treatment, animals were sacrificed at 1 h, 3 h, 6 h, 12 h, day 1, 2, 3, 5, and 7 ($n = 18$ mice/molecule/time point). Time-dependent MAC deposition, along with CCL2 and VEGF expression, was determined. Immunohistochemical staining of RPE-choroid-sclera flat mounts and semi-quantitative evaluation of a positive fluorescent signal for MAC demonstrated that MAC deposition increased significantly ($p < 0.05$) at 1 h post-laser treatment compared with naïve mice, peaked at day 3, and remained elevated until day 7 (Fig. 1, *A* and *B*). Results of quantitative real-time RT-PCR and ELISA revealed that in RPE-choroid, CCL2 mRNA (Fig. 1*C*) and protein (Fig. 1*D*) levels were significantly ($p < 0.05$) elevated at 3 h post-laser treatment and peaked at 12 h post-laser treatment relative to naïve mice. Compared with naïve animals, both mRNA (Fig. 1*E*) and protein (Fig. 1*F*) levels of VEGF remained unaltered until day 1 post-laser treatment as determined by real-time RT-PCR and ELISA, respectively. Levels of VEGF mRNA were significantly ($p < 0.05$) elevated at day 2 (Fig. 1*E*), whereas significantly ($p < 0.05$)

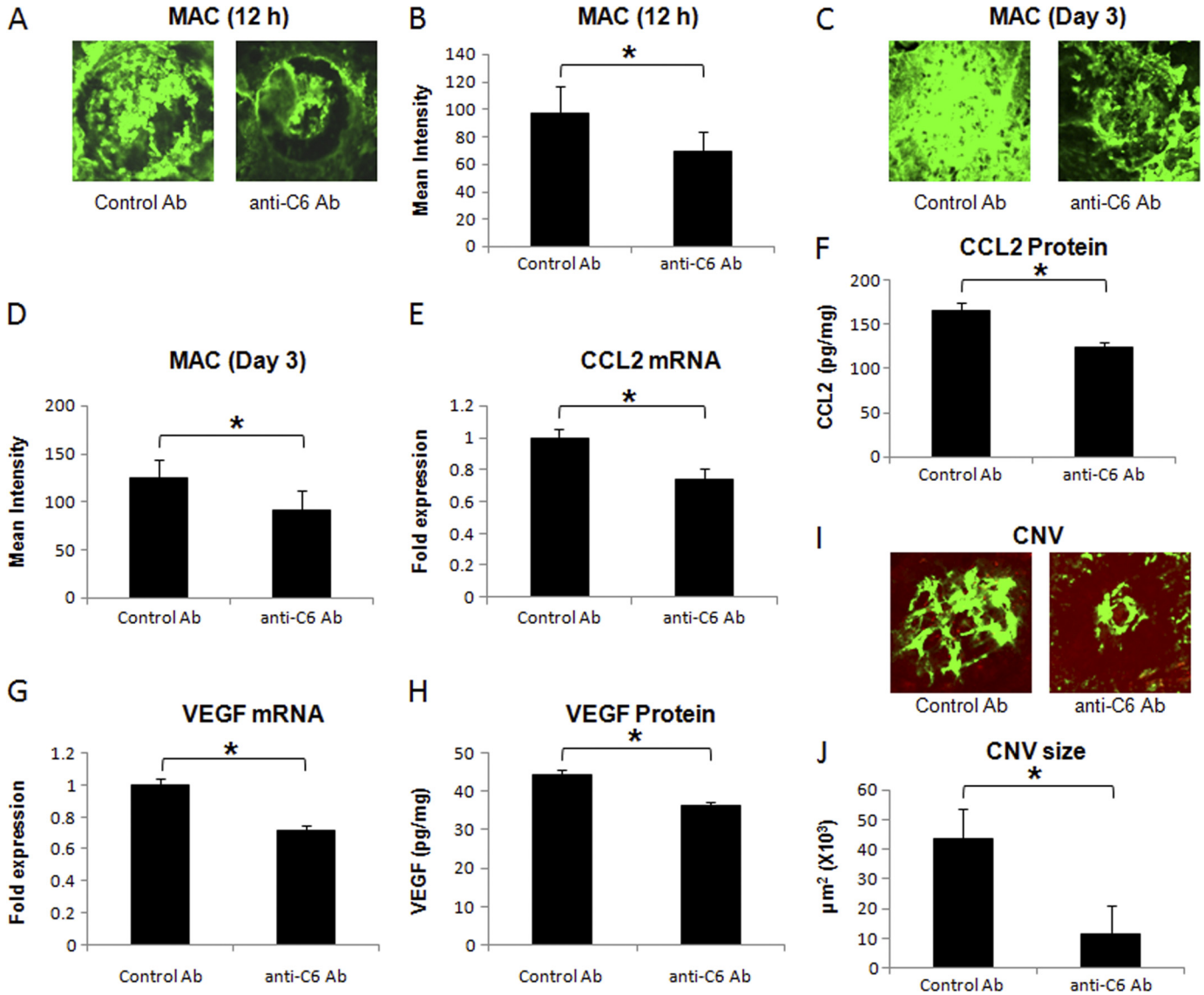

FIGURE 3. **Effect of subretinal administration of anti-murine C6 on MAC deposition, CCL2 expression, VEGF expression, and formation of CNV complex.** Representative confocal micrographs of RPE-choroid-sclera flat mounts immunostained for MAC at 12 h (*A*) and day 3 (*C*) post-laser treatment from mice injected with anti-murine C6 or control antibody via sub-retinal route. Graphs show semi-quantitative evaluation of positive fluorescent signal for MAC at 12 h (*B*) and at day 3 (*D*). CCL2 mRNA (*E*) and protein (*F*) levels were analyzed 12 h after laser treatment, whereas levels of VEGF mRNA (*G*) and protein (*H*) were determined at day 3 post-laser treatment by real-time RT-PCR and ELISA, respectively, in RPE-choroid of mice injected with anti-murine C6 or control antibody via subretinal route. Representative confocal microphotographs of RPE-choroid-sclera flat mounts with FITC-dextran perfused vessels (*green*) from C57BL/6 mice injected sub-retinally with anti-murine C6 or control antibody and sacrificed at day 7 post-laser treatment are shown (*I*). Cumulative data obtained by the quantification of the images are shown (*J*). Quantification and statistical analyses, including S.D. and Student's *t* test, were performed as described under "Experimental Procedures." All data are representative of three independent experiments. *, $p < 0.05$.

elevated VEGF protein levels were detected at day 3 post-laser treatment (Fig. 1*F*). CNV formation at above mentioned time points was also monitored. CNV was observed in most laser-treated spots at day 5 post-laser treatment, and the CNV complex was fully developed on day 7 (Fig. 1, *G* and *H*). Experiments were repeated three times with similar results.

Effect of MAC on CCL2 and VEGF

To investigate the effect of MAC inhibition *in vivo* on CCL2 and VEGF, C57BL/6 mice were injected with polyclonal anti-mouse C6 antibody systemically (i.p.) or locally (subretinal). Control animals received similar treatment with control antibody. The effect of anti-C6 antibody on complement system was determined by us in a previous study (27). The dose of this antibody for i.p. and sub-retinal injections used in the current study was determined in our pilot experiments by measuring the effect of each dose of antibody on CNV size in mice.

i.p. Injection—Systemic administration of the anti-C6 antibody significantly ($p < 0.05$) reduced the deposition of MAC within the laser spots at 12 h post-laser treatment (~ 20%, Fig. 2, *A* and *B*) and at day 3 (~45%, Fig. 2, *C* and *D*) compared with mice treated similarly with the control antibody (Fig. 2, *A* and *B*). Because the CCL2 level peaked at 12 h post-laser treatment, and VEGF levels were elevated on day 3 post-laser treatment (Fig. 1), we decided to study the effect of anti-C6 on CCL2 and VEGF at 12 h and day 3 post-laser treatment, respectively. At

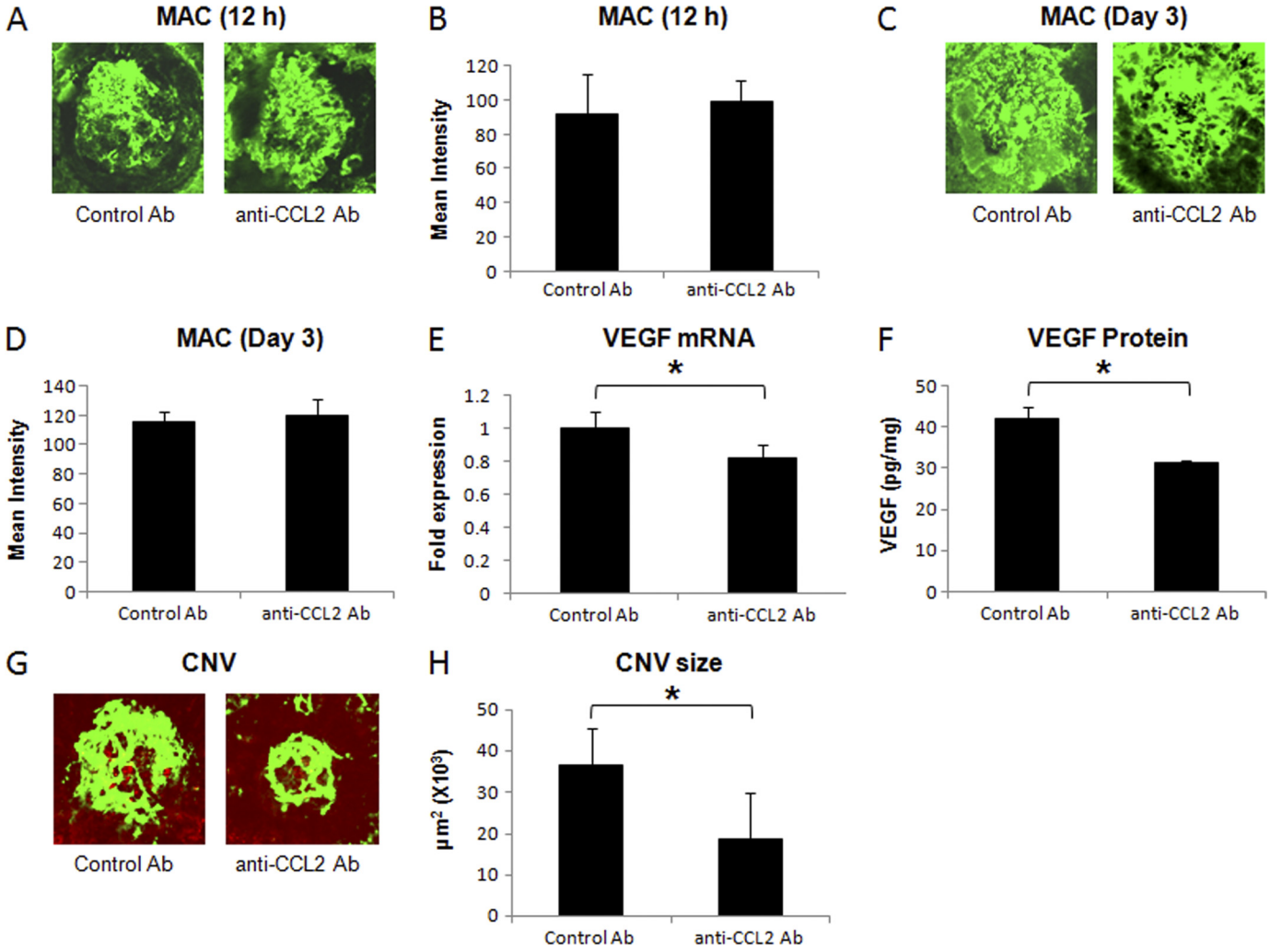

FIGURE 4. **Effect of i.p. injection of anti-murine CCL2 on MAC deposition, VEGF expression, and CNV formation.** *A* and *C* show representative confocal micrographs of RPE-choroid-sclera flat mounts immunostained for MAC at 12 h and day 3 post-laser treatment, respectively, from mice injected i.p. with anti-murine CCL2 or isotype control antibody. Semi-quantitative evaluation of positive fluorescent signal for MAC at 12 h (*B*) and at day 3 (*D*) is shown. VEGF mRNA (*E*) and protein (*F*) were analyzed at day 3 post-laser treatment by real-time RT-PCR and ELISA, respectively, in RPE-choroid of these animals. Representative confocal microphotographs of RPE-choroid-sclera flat mounts from C57BL/6 mice injected with anti-murine CCL2 or isotype control antibody and sacrificed at day 7 post-laser treatment are shown (*G*). Cumulative data obtained by the quantification of the images are shown (*H*). Quantification and statistical analyses, including S.D. and Student's *t* test, were performed as described under "Experimental Procedures." All data are representative of three independent experiments. *, $p < 0.05$.

12 h post-laser treatment, blocking MAC formation significantly ($p < 0.05$) decreased the expression of CCL2 (both mRNA and protein). Mice treated with anti-C6 antibody had significantly ($p < 0.05$) reduced (~30%) levels of CCL2 mRNA (Fig. 2*E*) and protein (Fig. 2*F*) compared with mice treated with control antibody. We noted that in anti-C6 treated mice, VEGF mRNA (Fig. 2*G*) and protein (Fig. 2*H*) levels were also significantly ($p < 0.05$) decreased (~ 25%) at day 3 post-laser treatment, and CNV was significantly ($p < 0.05$) inhibited (~77%) on day 7 post-laser treatment (Fig. 2, *I* and *J*) compared with control antibody-treated animals.

Subretinal Injection—In another set of experiments, local (*i.e.* ocular) MAC formation was inhibited by injecting anti-C6 antibody subretinally in the eye of C57BL/6 mice immediately after laser treatment.

We observed that subretinal injection of the anti-C6 antibody significantly ($p < 0.05$) decreased MAC deposition at 12 h (~29%, Fig. 3, *A* and *B*) and on day 3 (~26%, Fig. 3, *C* and *D*) post-laser treatment compared with treatment with control IgG. Treatment with anti-C6 also resulted in significantly ($p < 0.05$) reduced expression of CCL2 mRNA (~26%, Fig. 3*E*) and protein (~25%, Fig. 3*F*) at 12 h post-laser treatment, significantly ($p < 0.05$) reduced expression of VEGF mRNA (~29%, Fig. 3*G*) and protein (25%, Fig. 3*H*) on day 3 post-laser treatment and inhibited the formation of CNV complex (~73%, Fig. 3, *I* and *J*) at day 7 compared with the animals treated similarly with control antibody.

Collectively, our data demonstrate that both systemic and local inhibition of MAC down-regulates CCL2 as well as VEGF and inhibits the development of CNV complex. These results suggest that MAC is crucial for the expression of CCL2 and VEGF during laser-induced CNV.

Effect of CCL2 on MAC and VEGF

Experiments were performed to explore the effect of CCL2 neutralization on MAC and VEGF during laser-induced CNV

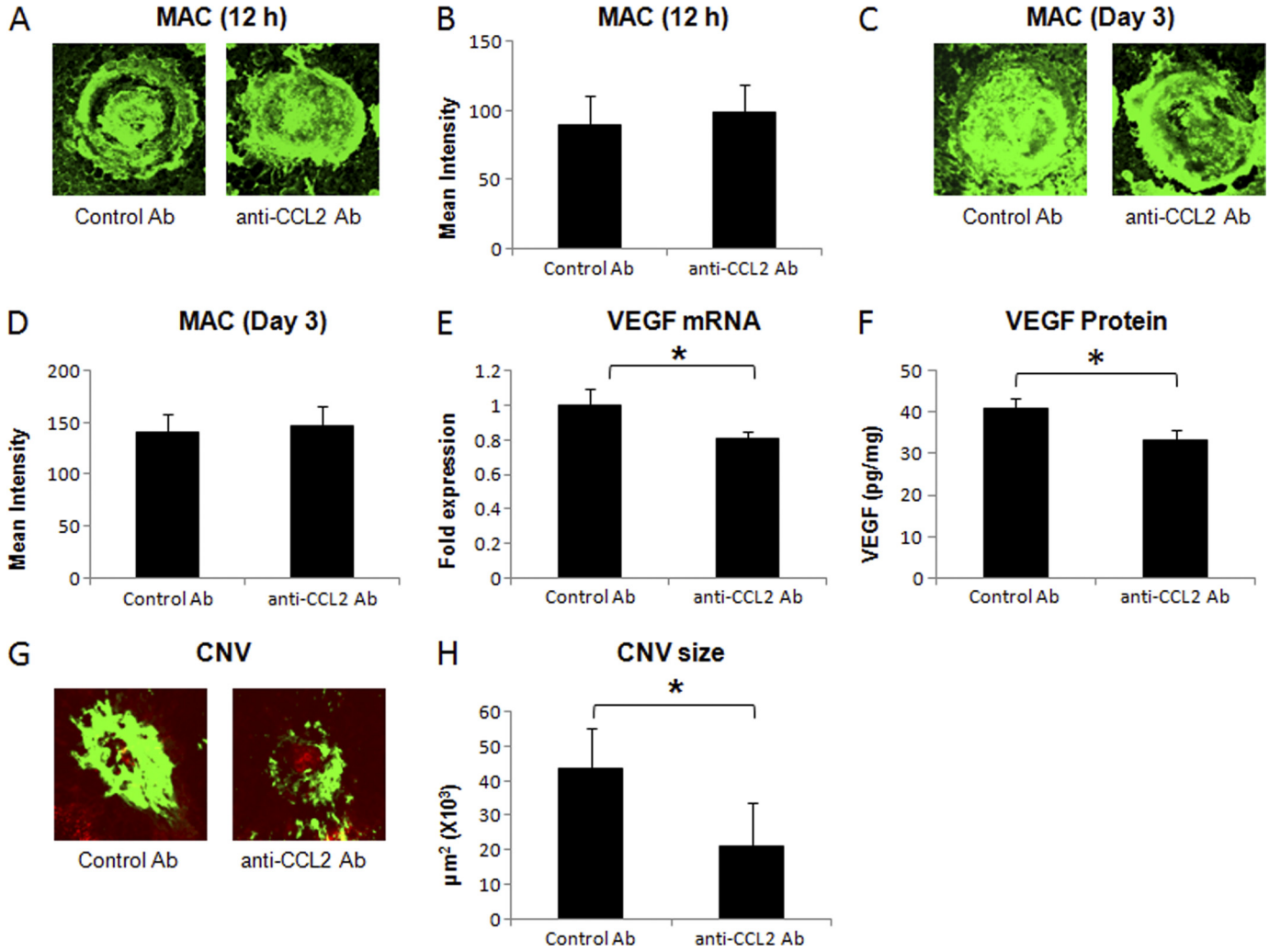

FIGURE 5. **Effect of subretinal administration of anti-murine CCL2 on MAC deposition, VEGF expression, and formation of CNV complex.** Representative confocal micrographs of RPE-choroid-sclera flat mounts immunostained for MAC at 12 h (*A*) and day 3 (*C*) post-laser treatment from mice injected with anti-murine CCL2 or isotype control antibody via subretinal route. Graphs show semi-quantitative evaluation of positive fluorescent signal for MAC at 12 h (*B*) and at day 3 (*D*). VEGF mRNA (*E*) and protein (*F*) were determined at day 3 post-laser treatment by real-time RT-PCR and ELISA, respectively, in RPE-choroid. Representative confocal microphotographs of RPE-choroid-sclera flat mounts from C57BL/6 mice injected sub-retinally with anti-murine CCL2 or isotype control antibody and sacrificed at day 7 post-laser treatment are shown (*G*). Cumulative data obtained by the quantification of the images are shown (*H*). Quantification and statistical analyses, including S.D. and Student's *t* test, were performed as described under "Experimental Procedures." All data are representative of three independent experiments. *, $p < 0.05$.

and CCL2 bioactivity was blocked *in vivo* by i.p. or subretinal injection of monoclonal anti-mouse CCL2 antibody. Control animals received similar treatment with isotype control antibody. Monoclonal anti-mouse CCL2 is reported to neutralize mouse CCL2 bioactivity by the manufacturer (R&D Systems) and the dose of this antibody for i.p. and sub-retinal injections used in the current study was determined in our pilot experiments by measuring the effect of each dose of antibody on the size of the CNV complex in mice.

i.p. Injection—C57BL/6 mice were injected with monoclonal anti-mouse CCL2 antibody or control rat IgG as described under "Experimental Procedures." Neutralization of CCL2 bioactivity did not alter the MAC deposition within laser spots both at 12 h (Fig. 4, *A* and *B*) and on day 3 post-laser treatment (Fig. 4, *C* and *D*). Levels of MAC in mice treated with anti-CCL2 were similar to those observed in the animals treated similarly with isotype control antibody at these time points (Fig. 4, *A*–*D*) Interestingly, treatment with anti-CCL2 antibody resulted in significantly ($p < 0.05$) reduced levels of VEGF mRNA (~18%, Fig. 4*E*) and VEGF protein (~ 26%, Fig. 4*F*) at day 3 post-laser treatment compared with mice treated with isotype control. Additionally, CNV formation was also inhibited in these animals by 49% at day 7 (Fig. 4, *G* and *H*).

Subretinal Injection—C57BL/6 mice were injected 10 μg of neutralizing antibody against mouse CCL2 immediately after laser treatment via subretinal route. Our results presented in Fig. 5 demonstrate that neutralization of CCL2 bioactivity within the mouse eye did not affect the MAC deposition in laser spots at 12 h (Fig. 5, *A* and *B*) and at day 3 (Fig. 5, *C* and *D*) post-laser treatment, and the levels of MAC in these animals were similar to those observed in the mice treated with isotype control antibody. However, VEGF expression was significantly ($p < 0.05$) reduced (~20%, Fig. 5, *E* and *F*) at day 3, and CNV formation at day 7 was inhibited (~51%) by treatment with anti-CCL2 (Fig. 5, *G* and *H*) compared with similar treatment with isotype control antibody.

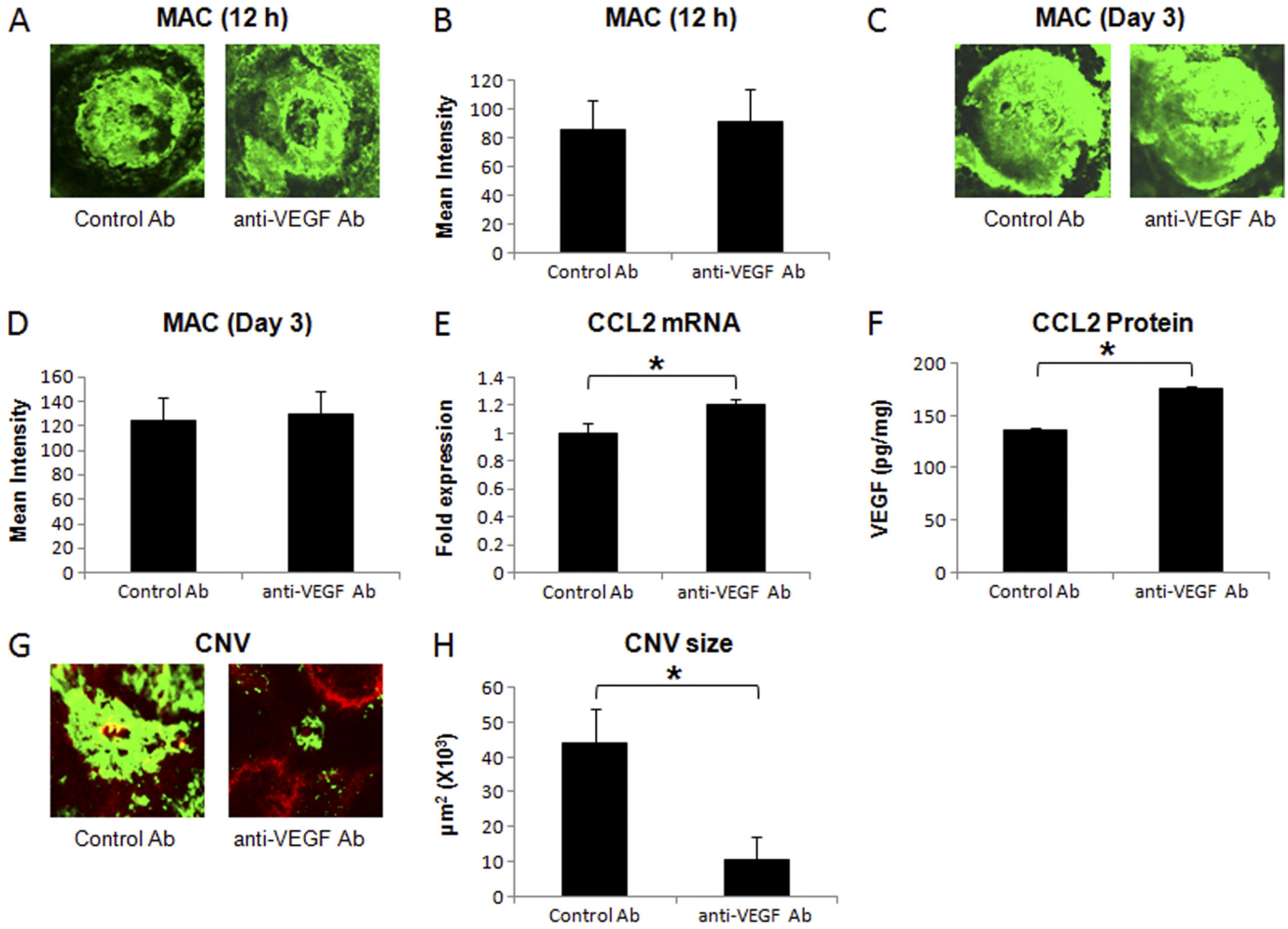

FIGURE 6. **Effect of i.p. injection of anti-murine VEGF on MAC deposition, CCL2 expression, and formation of CNV complex.** *A* and *C* show representative confocal micrographs of RPE-choroid-sclera flat mounts immunostained for MAC at 12 h and day 3 post-laser treatment, respectively, from mice injected i.p. with anti-murine VEGF or control antibody. Semi-quantitative evaluation of positive fluorescent signal for MAC at 12 h (*B*) and at day 3 (*D*) is shown. CCL2 mRNA (*E*) and protein (*F*) were analyzed at 12 h post-laser treatment by real-time RT-PCR and ELISA, respectively, in RPE-choroid of these animals. Representative confocal microphotographs of RPE-choroid-sclera flat mounts from C57BL/6 mice injected with anti-murine VEGF or control antibody and sacrificed at day 7 post-laser treatment are shown (*G*). *H* represents the cumulative data of CNV quantification. Quantification and statistical analyses, including S.D. and Student's *t* test, were performed as described under "Experimental Procedures." All data are representative of three independent experiments. *, $p < 0.05$.

Thus, the above-mentioned results demonstrate that the levels of VEGF were significantly reduced by interception of CCL2 bioactivity; however, MAC formation was not affected by this treatment. The formation of CNV complex was also inhibited in the animals treated with CCL2 antibody. Taken together, our results suggest that CCL2 expression is downstream to MAC deposition and upstream of VEGF expression during laser-induced CNV.

Effect of VEGF on MAC and CCL2

Experiments were performed to study the effect of VEGF neutralization on MAC and CCL2 during laser-induced CNV. The bioactivity of VEGF was blocked *in vivo* by i.p. or subretinal injection of polyclonal anti-mouse VEGF antibody. Control animals received similar treatment with control antibody. Polyclonal anti-mouse VEGF is reported to neutralize mouse VEGF bioactivity by the manufacturer (R&D Systems), and the dose of this antibody for ip and sub-retinal injections used in the current study was determined in our pilot experiments by measuring the effect of each dose of antibody on the size of the CNV complex in mice.

i.p. Injection—Animals injected with anti-VEGF antibody or control goat IgG (described under "Experimental Procedures") were sacrificed at 12 h, day 3, or day 7, and the harvested eyes were analyzed for MAC deposition, CCL2 expression, and CNV formation. As shown in Fig. 6, blocking VEGF bioactivity had no effect on MAC deposition at 12 h (Fig. 6, *A* and *B*) and day 3 (Fig. 6, *C* and *D*) post-laser treatment. Levels of MAC in mice treated with anti-VEGF were similar to those observed in the animals treated similarly with control antibody at these time points (Fig. 6, *A–D*). Interestingly, mice in which the VEGF bioactivity was blocked produced significantly ($p < 0.05$) more CCL2 mRNA (Fig. 6*E*) and protein (Fig. 6*F*) at 12 h post-laser treatment relative to control mice treated similarly with control antibody. On day 7 post-laser treatment, CNV formation was significantly ($p < 0.05$) inhibited (~77%) in anti-VEGF antibody-treated mice compared with the animals treated with control antibody (Fig. 6, *G* and *H*).

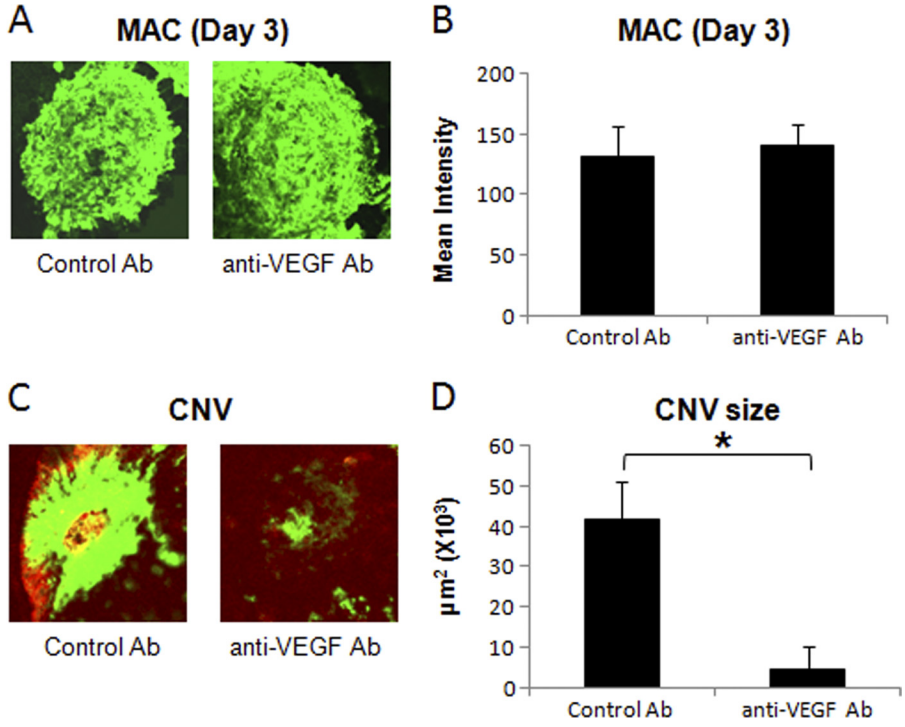

FIGURE 7. **Effect of subretinal administration of anti-murine VEGF on MAC deposition and formation of CNV complex.** Representative confocal micrographs of RPE-choroid-sclera flat mounts immunostained for MAC at day 3 (*A*) post-laser treatment from mice injected with anti-murine VEGF or control antibody via subretinal route. *B* represents semi-quantitative evaluation of positive fluorescent signal for MAC at this time point. Representative confocal microphotographs of RPE-choroid-sclera flat mounts from C57BL/6 mice injected subretinally with anti-murine VEGF or control antibody and sacrificed at day 7 post-laser treatment are shown (*C*). *D* shows the cumulative data of CNV quantification. Quantification and statistical analyses, including S.D. and Student's *t* test, were performed as described under "Experimental Procedures." All data are representative of three independent experiments. *, $p < 0.05$.

Subretinal Injection—Anti-VEGF antibody (15 μg) was injected via sub-retinal route into the eye of C57BL/6 mice on day 2 post-laser treatment to block VEGF bioactivity locally. Local blockade of VEGF function did not affect MAC deposition on day 3 post-laser treatment (Fig. 7, *A* and *B*), and the levels of MAC in these animals were similar to those observed in the mice treated with control antibody. However, treatment with anti-VEGF significantly inhibited (~89%) CNV formation on day 7 post-laser treatment compared with the mice treated with control antibody (Fig. 7, *C* and *D*). Because CCL2 levels peaked at 12 h, declined at day 1 post-laser treatment, and subretinal injection of anti-VEGF was given at day 2 post-laser treatment, we could not study the effect of subretinal anti-VEGF on CCL2 expression.

Taken together, our results reveal that during laser-induced CNV, MAC deposition precedes CCL2, and VEGF expression and these molecules are formed and/or expressed in the following order: MAC → CCL2 → VEGF. Our results further demonstrate that during the course of laser-induced CNV, MAC regulates CCL2 and VEGF expression. MAC facilitates choroidal angiogenesis by directly up-regulating VEGF or by up-regulating VEGF through its effect on CCL2 (Fig. 8).

DISCUSSION

CNV-associated with wet type (exudative) AMD leads to catastrophic loss of central vision among the elderly worldwide (1–5, 53, 54). Currently available agents as well as procedures for the treatment of exudative AMD have limited efficacy and are associated with significant ocular complications (55–57). Therefore, studies exploring the molecular mechanisms involved in CNV formation are essential to gain insight into the pathogenesis of CNV and are required for the development of effective therapy for this blinding disease. Over the years, experimental CNV induced by laser photocoagulation in mice has allowed the investigators to understand the pathogenesis as well as development and progression of CNV (27–32, 50, 51).

Using an animal model of laser-induced CNV, we have previously reported a correlation between MAC generation (as a result of complement activation via the alternative pathway) and the release of angiogenic growth factors, VEGF, basic fibroblast growth factors, and TGF-β, during laser-induced CNV (28, 29). Studies reported in the literature have indicated a possible role of chemokines in AMD (33–35, 58, 59). Furthermore, several studies have suggested that the expression of various chemokines can be regulated by complement activation products, including MAC (39–42). It is also known that various chemokines can modulate the levels of growth factors (43–46). However, the link between MAC, chemokines, and growth factors in laser-induced CNV is not elucidated thus far. In the present study, we investigated whether the effect of MAC on the induction and/or release of angiogenic growth factors is mediated by chemokines in mouse model of laser-induced CNV. This study provides evidence for the first time that MAC regulates CNV by modulating the expression of chemokines and angiogenic growth factors.

We hypothesized that MAC will modulate the production and/or secretion of chemokine and will facilitate angiogenesis

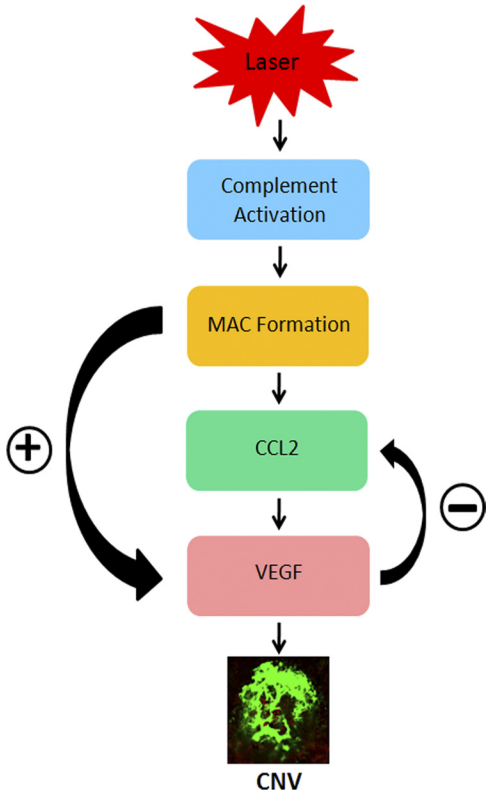

FIGURE 8. **A schematic of interrelationship between MAC, CCL2, and VEGF during laser-induced CNV.** Laser treatment leads to complement activation within the posterior segment of the eye which results in MAC deposition within the laser spots. MAC facilitates choroidal angiogenesis by directly up-regulating VEGF or by up-regulating VEGF through CCL2. Our data suggest that there are reciprocal interactions between CCL2 and VEGF.

by inducing angiogenic growth factors in the laser-induced CNV mouse model. To test this hypothesis, a series of experiments were performed, and we focused our attention on CCL2 and VEGF. This is because the evidence in the literature provides ample evidence that VEGF is a major factor in the development of CNV (60–62) and CCL2 has been reported to play an important role in AMD (33–35).

The first experiments were conducted to determine time-dependent expression of MAC, CCL2, and VEGF after laser photocoagulation. We found that MAC deposition started to increase as early as 1 h post-laser treatment, CCL2 levels increased at 3 h post-laser treatment, and VEGF increased significantly at days 2–3 post-laser treatment. CNV complex started to form on day 5 post-laser treatment, and CNV was fully developed by day 7. Collectively, these results suggest that in the laser treatment-induced mouse model CNV formation takes place in the following order: MAC deposition → CCL2 expression → VEGF production → CNV formation.

Having demonstrated sequence of MAC, CCL2, and VEGF expression during laser-induced CNV, we sought to establish a link between MAC, CCL2, and VEGF and used neutralizing antibodies against C6, CCL2, and VEGF to explore the cross-talk between MAC, CCL2, and VEGF in this animal model. We first blocked MAC formation using an anti-mouse C6 antibody. MAC is a multimolecular complex composed of five complement proteins, C5b, C6, C7, C8, and C9 (C5b-9). MAC cannot be fully formed and will not be functional if the function of any component comprising MAC is blocked (63–65). By giving systemic injections of anti-mouse C6 antibody, we successfully inhibited MAC formation *in vivo* in the laser-induced CNV mouse model. Decreased MAC formation resulted in reduced expression of CCL2 and VEGF (both mRNA and protein) and inhibited CNV formation. Local blocking (by subretinal injection) of MAC had similar effect. Next, we neutralized the bioactivity of CCL2 *in vivo* (both systemically and locally) using an anti-mouse CCL2 antibody, and explored whether loss of CCL2 function affects MAC deposition, VEGF expression, and CNV formation. Blocking of CCL2 function inhibited VEGF expression and CNV formation; however, it had no effect on MAC deposition in the laser spots. Finally, we blocked the bioactivity of VEGF using neutralizing antibody against mouse VEGF. Systemic and local neutralization of the VEGF bioactivity inhibited CNV formation significantly but did not affect MAC deposition. Interestingly, neutralization of VEGF bioactivity leads to increased CCL2 expression, thus suggesting that VEGF expression may have a negative feedback effect on CCL2 expression. CCL2 has been reported to have a bidirectional relationship with VEGF (46, 66–68).

Together, our results demonstrate that MAC is an upstream mediator and effect of MAC on the development of CNV can be attributed to its direct effect on VEGF as well as its effect on VEGF that is mediated by CCL2 (Fig. 8). Although, our study focused on CCL2 and VEGF, we cannot rule out the role of potential cross-talk between MAC and other chemokines as well as growth factors. Several chemokines such as IL-8 (KC in mouse) and angiogenic growth factors modulated by MAC have been implicated in the pathogenesis of AMD (27–29, 69, 70). In conclusion, our study provides evidence for the first time that the interactions between MAC, CCL2, and VEGF are crucial in the pathogenesis of CNV. There is a dynamic balance between MAC, chemokine (CCL2), and angiogenic growth factor (VEGF) in mouse model of laser-induced CNV (Fig. 8). The results presented here describe important immune interactions that occur during the development of laser-induced CNV. In terms of therapy, understanding the mechanisms of action of different immunological factors may enable multiple approaches to treat CNV or neovascular AMD.

REFERENCES

1. O'Shea, J. G. (1996) *Med. J. Aust.* **165,** 561–564
2. Nussenblatt, R. B., Liu, B., and Li, Z. (2009) *Curr. Opin. Investig. Drugs* **10,** 434–442
3. Chappelow, A. V., and Kaiser, P. K. (2008) *Drugs* **68,** 1029–1036
4. Rohrer, B., Long, Q., Coughlin, B., Wilson, R. B., Huang, Y., Qiao, F., Tang, P. H., Kunchithapautham, K., Gilkeson, G. S., and Tomlinson, S. (2009) *Invest. Ophthalmol. Vis. Sci.* **50,** 3056–3064
5. Thurman, J. M., Renner, B., Kunchithapautham, K., Ferreira, V. P., Pangburn, M. K., Ablonczy, Z., Tomlinson, S., Holers, V. M., and Rohrer, B. (2009) *J. Biol. Chem.* **284,** 16939–16947
6. de Jong, P. T. (2006) *N. Engl. J. Med.* **355,** 1474–1485
7. Ozkiris, A. (2010) *Expert. Opin. Ther. Pat.* **20,** 103–118
8. Miller, D. G., and Singerman, L. J. (2006) *Optom. Vis. Sci.* **83,** 316–325
9. Michels, S., Schmidt-Erfurth, U., and Rosenfeld, P. J. (2006) *Expert. Opin. Investig. Drugs* **15,** 779–793
10. Andreoli, C. M., and Miller, J. W. (2007) *Curr. Opin. Ophthalmol.* **18,** 502–508
11. Liutkeviciene, R., Lesauskaite, V., Asmoniene, V., Zaliūniene, D., and Jasinskas, V. (2010) *Medicina* **46,** 89–94

12. Sepp, T., Khan, J. C., Thurlby, D. A., Shahid, H., Clayton, D. G., Moore, A. T., Bird, A. C., and Yates, J. R. (2006) *Invest. Ophthalmol. Vis. Sci.* **47,** 536–540
13. Hogg, R. E., Woodside, J. V., Gilchrist, S. E., Graydon, R., Fletcher, A. E., Chan, W., Knox, A., Cartmill, B., and Chakravarthy, U. (2008) *Ophthalmology* **115,** 1046–1052.e2
14. Suñer, I. J., Espinosa-Heidmann, D. G., Marin-Castano, M. E., Hernandez, E. P., Pereira-Simon, S., and Cousins, S. W. (2004) *Invest. Ophthalmol. Vis. Sci.* **45,** 311–317
15. Kaliappan, S., Jha, P., Lyzogubov, V. V., Tytarenko, R. G., Bora, N. S., and Bora, P. S. (2008) *FEBS Lett.* **582,** 3451–3458
16. Anderson, D. H., Radeke, M. J., Gallo, N. B., Chapin, E. A., Johnson, P. T., Curletti, C. R., Hancox, L. S., Hu, J., Ebright, J. N., Malek, G., Hauser, M. A., Rickman, C. B., Bok, D., Hageman, G. S., and Johnson, L. V. (2010) *Prog. Retin. Eye Res.* **29,** 95–112
17. Klein, R. J., Zeiss, C., Chew, E. Y., Tsai, J. Y., Sackler, R. S., Haynes, C., Henning, A. K., SanGiovanni, J. P., Mane, S. M., Mayne, S. T., Bracken, M. B., Ferris, F. L., Ott, J., Barnstable, C., and Hoh, J. (2005) *Science* **308,** 385–389
18. Edwards, A. O., Ritter, R., 3rd, Abel, K. J., Manning, A., Panhuysen, C., and Farrer, L. A. (2005) *Science* **308,** 421–424
19. Haines, J. L., Hauser, M. A., Schmidt, S., Scott, W. K., Olson, L. M., Gallins, P., Spencer, K. L., Kwan, S. Y., Noureddine, M., Gilbert, J. R., Schnetz-Boutaud, N., Agarwal, A., Postel, E. A., and Pericak-Vance, M. A. (2005) *Science* **308,** 419–421
20. Bora, N. S., Jha, P., and Bora, P. S. (2008) *Semin. Immunopathol.* **30,** 85–95
21. Jha, P., Bora, P. S., and Bora, N. S. (2007) *Mol. Immunol.* **44,** 3901–3908
22. Sohn, J. H., Bora, P. S., Suk, H. J., Molina, H., Kaplan, H. J., and Bora, N. S. (2003) *Nat. Med.* **9,** 206–212
23. Rambach, G., Würzner, R., and Speth, C. (2008) *Contrib. Microbiol.* **15,** 78–100
24. Dunkelberger, J. R., and Song, W. C. (2010) *Mol. Immunol.* **47,** 2176–2186
25. Kemper, C., and Atkinson, J. P. (2007) *Nat. Rev. Immunol.* **7,** 9–18
26. Dunkelberger, J. R., and Song, W. C. (2010) *Cell Res.* **20,** 34–50
27. Bora, P. S., Sohn, J. H., Cruz, J. M., Jha, P., Nishihori, H., Wang, Y., Kaliappan, S., Kaplan, H. J., and Bora, N. S. (2005) *J. Immunol.* **174,** 491–497
28. Bora, N. S., Kaliappan, S., Jha, P., Xu, Q., Sohn, J. H., Dhaulakhandi, D. B., Kaplan, H. J., and Bora, P. S. (2006) *J. Immunol.* **177,** 1872–1878
29. Bora, N. S., Kaliappan, S., Jha, P., Xu, Q., Sivasankar, B., Harris, C. L., Morgan, B. P., and Bora, P. S. (2007) *J. Immunol.* **178,** 1783–1790
30. Ashikari, M., Tokoro, M., Itaya, M., Nozaki, M., and Ogura, Y. (2010) *Invest. Ophthalmol. Vis. Sci.* **51,** 3820–3824
31. Inomata, Y., Fukushima, M., Hara, R., Takahashi, E., Honjo, M., Koga, T., Kawaji, T., Satoh, H., Takeya, M., Sawamura, T., and Tanihara, H. (2009) *Invest. Ophthalmol. Vis. Sci.* **50,** 3970–3976
32. Chung, E. J., Yoo, S., Lim, H. J., Byeon, S. H., Lee, J. H., and Koh, H. J. (2009) *Br. J. Ophthalmol.* **93,** 958–963
33. Ambati, J., Anand, A., Fernandez, S., Sakurai, E., Lynn, B. C., Kuziel, W. A., Rollins, B. J., and Ambati, B. K. (2003) *Nat. Med.* **9,** 1390–1397
34. Yamada, K., Sakurai, E., Itaya, M., Yamasaki, S., and Ogura, Y. (2007) *Invest. Ophthalmol. Vis. Sci.* **48,** 1839–1843
35. Chan, C. C., Ross, R. J., Shen, D., Ding, X., Majumdar, Z., Bojanowski, C. M., Zhou, M., Salem, N., Jr., Bonner, R., and Tuo, J. (2008) *Ophthalmic. Res.* **40,** 124–128
36. Luhmann, U. F., Robbie, S., Munro, P. M., Barker, S. E., Duran, Y., Luong, V., Fitzke, F. W., Bainbridge, J. W., Ali, R. R., and MacLaren, R. E. (2009) *Invest. Ophthalmol. Vis. Sci.* **50,** 5934–5943
37. Daly, C., and Rollins, B. J. (2003) *Microcirculation* **10,** 247–257
38. Conductier, G., Blondeau, N., Guyon, A., Nahon, J. L., and Rovère, C. (2010) *J. Neuroimmunol.* **224,** 93–100
39. Kilgore, K. S., Flory, C. M., Miller, B. F., Evans, V. M., and Warren, J. S. (1996) *Am. J. Pathol.* **149,** 953–961
40. Risnes, I., Ueland, T., Aukrust, P., Lundblad, R., Baksaas, S. T., Mollnes, T. E., and Svennevig, J. L. (2003) *Ann. Thorac. Surg.* **75,** 981–985
41. Selvan, R. S., Kapadia, H. B., and Platt, J. L. (1998) *J. Immunol.* **161,** 4388–4395
42. Torzewski, J., Oldroyd, R., Lachmann, P., Fitzsimmons, C., Proudfoot, D., and Bowyer, D. (1996) *Arterioscler. Thromb. Vasc. Biol.* **16,** 673–677
43. Rosenkilde, M. M., and Schwartz, T. W. (2004) *APMIS* **112,** 481–495
44. Hwang, J., Son, K. N., Kim, C. W., Ko, J., Na, D. S., Kwon, B. S., Gho, Y. S., and Kim, J. (2005) *Cytokine* **30,** 254–263
45. Tettamanti, G., Malagoli, D., Benelli, R., Albini, A., Grimaldi, A., Perletti, G., Noonan, D. M., de Eguileor, M., and Ottaviani, E. (2006) *Curr. Med. Chem.* **13,** 2737–2750
46. Itaya, M., Sakurai, E., Nozaki, M., Yamada, K., Yamasaki, S., Asai, K., and Ogura, Y. (2007) *Invest. Ophthalmol. Vis. Sci.* **48,** 5677–5683
47. Miller, H., Miller, B., Ishibashi, T., and Ryan, S. J. (1990) *Invest. Ophthalmol. Vis. Sci.* **31,** 899–908
48. Campochiaro, P. A. (2000) *J. Cell Physiol.* **184,** 301–310
49. Edelman, J. L., and Castro, M. R. (2000) *Exp. Eye Res.* **71,** 523–533
50. Lyzogubov, V. V., Tytarenko, R. G., Jha, P., Liu, J., Bora, N. S., and Bora, P. S. (2010) *Am. J. Pathol.* **177,** 1870–1880
51. Bora, N. S., Jha, P., Lyzogubov, V. V., Kaliappan, S., Liu, J., Tytarenko, R. G., Fraser, D. A., Morgan, B. P., and Bora, P. S. (2010) *J. Biol. Chem.* **285,** 33826–33833
52. Bora, P. S., Hu, Z., Tezel, T. H., Sohn, J. H., Kang, S. G., Cruz, J. M., Bora, N. S., Garen, A., and Kaplan, H. J. (2003) *Proc. Natl. Acad. Sci. U.S.A.* **100,** 2679–2684
53. Bressler, S. B. (2009) *Ophthalmology* **116,** S1–7
54. Barakat, M. R., and Kaiser, P. K. (2009) *Expert. Opin. Investig. Drugs* **18,** 637–646
55. Joussen, A. M., and Bornfeld, N. (2009) *Dtsch. Arztebl. Int.* **106,** 312–317
56. Prasad, P. S., Schwartz, S. D., and Hubschman, J. P. (2010) *Maturitas* **66,** 46–50
57. Augustin, A. J., Scholl, S., and Kirchhof, J. (2009) *Clin. Ophthalmol.* **3,** 175–182
58. Wang, Y., Bian, Z. M., Yu, W. Z., Yan, Z., Chen, W. C., and Li, X. X. (2010) *Exp. Eye Res.* **91,** 135–142
59. Wang, J., Ohno-Matsui, K., Yoshida, T., Shimada, N., Ichinose, S., Sato, T., Mochizuki, M., and Morita, I. (2009) *J. Cell Physiol.* **220,** 119–128
60. Cohen, S. Y. (2009) *Retina* **29,** 1062–1066
61. Kim, S. J., Toma, H. S., Barnett, J. M., and Penn, J. S. (2010) *Exp. Eye Res.* **91,** 537–543
62. Takahashi, H., Ishizaki, H., Tahara, H., Tamaki, Y., and Yanagi, Y. (2008) *Invest. Ophthalmol. Vis. Sci.* **49,** 2143–2147
63. Esser, A. F. (1994) *Toxicology* **87,** 229–247
64. Podack, E. R., and Tschopp, J. (1984) *Mol. Immunol.* **21,** 589–603
65. Brannen, C. L., and Sodetz, J. M. (2007) *Mol. Immunol.* **44,** 960–965
66. Marumo, T., Schini-Kerth, V. B., and Busse, R. (1999) *Diabetes* **48,** 1131–1137
67. Yamada, M., Kim, S., Egashira, K., Takeya, M., Ikeda, T., Mimura, O., and Iwao, H. (2003) *Arterioscler. Thromb. Vasc. Biol.* **23,** 1996–2001
68. Hong, K. H., Ryu, J., and Han, K. H. (2005) *Blood* **105,** 1405–1407
69. Goverdhan, S. V., Ennis, S., Hannan, S. R., Madhusudhana, K. C., Cree, A. J., Luff, A. J., and Lotery, A. J. (2008) *Br. J. Ophthalmol.* **92,** 537–540
70. Tsai, Y. Y., Lin, J. M., Wan, L., Lin, H. J., Tsai, Y., Lee, C. C., Tsai, C. H., Tsai, F. J., and Tseng, S. H. (2008) *Invest. Ophthalmol. Vis. Sci.* **49,** 693–698